Desalination and Water Treatment
www.deswater.com

doi:10.5004/dwt.2018.22137

107 (2018) 109–117
March

Oxidation performance of $Fe^0/Na_2S_2O_8$ process for the treatment of landfill leachate biochemical effluent as well as activator characterization

Zhanmeng Liu*, Xian Li, Fengping Hu*, Peng Zhan

School of Civil Engineering and Architecture, East China Jiao Tong University, Nanchang, 330013, China, Tel. +86 13576060580, email: ustblzm@sina.com (Z. Liu), lxlucky2017@qq.com (X. Li), 1536430581@qq.com (F. Hu), 821564310@qq.com (P. Zhan)

Received 25 September 2017; Accepted 1 March 2018

ABSTRACT

The aim of the present work was to study the oxidation performance as well as activator characterization of $Fe^0/Na_2S_2O_8$ system for the treatment of effluent from landfill leachate biochemical process. A typical persulfate (PS), $Na_2S_2O_8$ was activated by zero-valent iron (Fe^o) for the generation of the sulfate radical ($SO_4^{-}\cdot$) to oxidize the residual pollutants in landfill leachate biochemical effluent. The effect of various variables including $Na_2S_2O_8$ dosage, Fe^o dosage, pH value, and reaction time on the oxidation efficiency were investigated. The results indicated that the pollutants can be degraded efficiently by the $Fe^o/Na_2S_2O_8$ system. Under the working conditions of 2.5 g/L $Na_2S_2O_8$ dosage, 0.5 g/L Fe^o dosage, pH 7, and 12 h reaction time, the removal rates of COD and chroma reached up to 71% and 90%, respectively. Three-dimensional excitation emission matrix fluorescence spectrum (3DEEMFS), ultraviolet-visible spectrum (UV-vis), and Fourier Transform infrared spectrum (FTIR) illustrated that the pollution level of dissolved organic matters (DOM) in the wastewater samples which had been disposed by the $Fe^o/Na_2S_2O_8$ system and the humic acids were degraded into the small molecules of fulvic acid. The micro morphology of Fe^o was characterized using X-ray diffraction pattern (XRD), and Scanning electron microscope spectral (SEM). After reaction, it can be found a large amount of snowflake-like which contained iron oxide attached onto the surface of nano-Fe_3O_4.

Keywords: Leachate biochemical effluent; Micro morphology; Spectroscopy; Sulfate radical; Zero-valent iron

1. Introduction

Landfill leachate is a type of liquid pollutant, in which the ingredient is singularly complex, and has been included in the "black list" in China. Nowadays, landfill leachate as a mainly potential pollution source of surface water and groundwater is seriously threatening the safety of urban water environment. Therefore, the treatment of landfill leachate has attracted a lot of attentions from researchers in the field of sewage treatment in recent years. Moreover, the treatment processes should be able to have effective efficiencies on the treatment of landfill leachate and avoid secondary pollution as much as possible. Biological technology, given its unique advantages, particularly its operating costs lower than that of other treatment methods, has become the most preferred and most widely used one for landfill leachate treatment [1]. However, after treatment by the biological process, there are still many residual persistent pollutants in the effluent, which is a significant challenge for urban water environment and the wastewater samples need to be further treated. Advanced oxidation processes (AOPs), including electro catalytic oxidation [2,3], wet air oxidation [4,5], microwave oxidation [6], ozonation [7], Fenton [8] or oxidation like Fenton [9], as well as their involved combination [10], have been widely applied in the treatment of wastewater containing different organic compounds that are non-biodegradable and/or toxic to microorganisms. The potential advantages of advanced oxidation in the field of wastewater treatment have been widely concerned, and many researchers have confirmed that the main mechanism is the oxidation of ·OH (hydroxyl radical).

*Corresponding author.

In recent years, $SO_4^{-}\cdot$ oxidation has drawn increasing attention in the treatment of refractory wastewater and it is deemed to be a promising novel advanced oxidation technology [11]. It has been reported that the $SO_4^{-}\cdot$ are more selective than the ·OH for the oxidation of organic pollutants. Furthermore, compared with the ·OH, the half-life of $SO_4^{-}\cdot$ is up to 4s, which have adequate time to contact with contaminants and can achieve its purpose for oxidation [12]. Previous studies have indicated that a broad spectra of organic pollutants can be rapidly degraded via $SO_4^{-}\cdot$ oxidation [13]. Because of higher oxidation/reduction potential (ORP) of $SO_4^{-}\cdot$ (2.6 V) than that of persulfate anions ($S_2O_8^{2-}$) (2.1 V), the $SO_4^{-}\cdot$ oxidation technology has a strong oxidative capacity, as well as its low cost, with both two characteristics which facilitates its potential application in refractory wastewater treatment [14].

Persulfate is commonly used as a source of the $SO_4^{-}\cdot$ in laboratory studies and field applications based on its relatively high stability, solubility, and low cost, and often used in in-situ chemical oxidation [15]. However, oxidation by persulfates is ineffective under room temperature, and it always need to be activated for powerful $SO_4^{-}\cdot$ to oxidize the DOM in the wastewater. Activation of persulfate can be conducted by various methods, such as heat [16], transition metal ions [17], or UV light [5]. Using transition metal ions for the activation of persulfate is the commonly used one.

Applying Fe^o to wastewater treatment has become a research hot spot in recent years. When using Fe^o alone to deal with wastewater contamination, it has all functions including adsorption, coagulation, and electro chemistry, etc. [18–20]. The functions mentioned which can degrade COD, TOC in water, but the ability of degradation is limited and costly, so using Fe^o alone is unsuitable for the practical wastewater treatment [21].

Analogous to transitional metal ions, Fe^o, as a heterogeneous catalyst, can also activate PS to generated $SO_4^{-}\cdot$ at an ambient temperature [22]. Fe^o, as an iron source, may gradually release Fe^{2+} so that Fe^{2+} induced scavenging is minimal and the production of $SO_4^{-}\cdot$ proceeds during a relatively long time, which made it possible that the time is adequate for the contact reaction between $SO_4^{-}\cdot$ and organic contaminants. However, using Fe^{2+}/PS system to deal with polluted water, it can cause the reduction of removal efficiency and the deterioration of the wastewater quality as a result of the side reaction between Fe^{2+} and $SO_4^{-}\cdot$ with dosing Fe^{2+} directly [23]. What's more, heterogeneous catalyst Fe^0 can be recycled to reduce the treatment cost and avoid the secondary pollution caused by interfering ions. Oh et al. [24] had used different valence state of iron to activate persulfate and degrade 2,4-dinitrotoluene, the results found that the Fe^o/PS system is more excellent than that of the Fe^{2+}/PS system, not only in the effect of treatment but also in steadiness.

Although Fe^o/PS system has been widely used for various wastewater treatments, there is almost no report about the combined system used for treatment in the field of landfill leachate. The aims of this study were to (1) investigate the various variables (including $Na_2S_2O_8$ dosage, Fe^o dosage, pH value, and reaction time) on the removal efficiency of COD and chroma; (2) elucidate the mechanism of COD and chroma reduce through the analysis of 3DEEMFS, and assist with UV-vis and FTIR analyses for guarantee of the organic matters with high macromolecule weight degraded indeed into small molecular organics after treatment of Fe^o/PS system; (3) analyze the micro morphology of Fe^o before and after treatment by XRD and SEM, and further illustrate the mechanism of COD and chroma removal.

2. Materials and methods

2.1. Characteristics of wastewater samples

The experimental wastewater samples of leachate biochemical effluent was mature leachate leachated from the domestic garbage landfilled over 10 years, which were taken from the equalization storage pond of a municipal solid waste landfill disposal plant in Nanchang City, Jiangxi Province, PR China. During each sampling, 60 L of landfill leachate was collected in the polyethylene bottles pretreated by acid, and then transport to the laboratory, stored in a refrigerator at 4ºC. The characteristics of wastewater sample are as follows: the color is brown and no obvious odor, the pH is about 5.5–6.5, the COD content is 700–1300 mg/L, and the chroma is 620–720 times.

2.2. Materials

The chemical reagents used in this paper were all analytical grade except Fe^o powder. The Fe^o powder with 1.426 m^2/g BET surface was obtained from Shanghai No. 2 Metallurgical Plant. The persulfate ($Na_2S_2O_8$) and sodium hydroxide (NaOH) was purchased from Tianjin Hengxing Chemical Reagent Manufacturing Co., Ltd. Hydrochloric acid (HCl, 37% Wt) gained from Changzhou Yuantong Fine Chemical Co., Ltd., Jiangsu.

All reagents used were of analytical grade, and distilled water was used to prepare all aqueous solution.

2.3. Experimental procedures

Stock solutions of NaOH (25% Wt, dissolving 25 g NaOH in the 100 ml distilled water) and HCl (10% Wt, adding 200 ml 35% Wt HCl to 500 ml distilled water) were prepared prior to each batch experiment for adjusting pH value of wastewater samples. Batch experiments were conducted in 250 ml conical flask which contained 100 ml leachate biochemical effluent. First, the pH value of them was adjusted with our pre-prepared stock solutions to meet different experimental requirements. Second, appropriate amounts of $Na_2S_2O_8$, as an oxidant, were dosed into the leachate and made them mixed quickly with wastewater samples. Then the mixed solution subsequently added Fe^0 powder to activate persulfate for powerful sulfate radical, and placing conical flasks in a constant temperature oscillator (*Model SHZ-A*, Shanghai Jia Exhibition Equipment Co., Ltd.) with setting the temperature of 25ºC and rotating at the speed of 130 rpm. After reacting for a certain time, the mixed solution was added NaOH (25% Wt) to adjust pH value to alkalescence for better flocculated performance and minimizing the influence of iron flocculant on the removal of chroma. The supernatant based on above steps was collected for centrifugation at the speed of 3000 rpm for 15 min. With-

out any agitation and settled for a certain time (2 h), the supernatant was withdrawn after centrifugation and was used for chemical analysis.

2.4. Analytical methods

The COD and chroma were measured according to the Standard Methods for the Examination of Water and Wastewater established by the China Environmental Protection Agency. The pH was measured using a pH-meter (model PHS-3C). The chemical reagents used in this study were all of analytical grade. All samples were analyzed at a room temperature and the results were based on triplicate analysis.

2.4.1. 3DEEMFS

The 3DEEMFS of wastewater samples before and after treatment was determined using a fluorescence spectrophotometer (Hitachi F-2000). The filtered sample was scanned in a 1 cm quartz cell at excitation and emission ranges from 220 nm to 450 nm and from 220 nm to 600 nm, respectively.

2.4.2. UV-vis

The ultraviolet absorption spectrum of wastewater samples before and after treatment was determined using an ultraviolet Spectrophotometer (model UV-2450). The filtered sample was scanned in a 1 cm quartz cell in the range of 190–450 nm.

2.4.3. FTIR

The FTIR of wastewater samples before and after treatment was determined using an infrared spectrophotometer (model D/Max-RC). Briefly, the wastewater samples before and after treatment were dried and mixed with pre-dried KBr powder respectively, and then were both sufficiently ground and pressed in a pellet which was suitable for FTIR analysis. FTIR spectroscopy was then conducted and the spectra were in the range of 4000–400 cm^{-1}.

2.4.4. XRD

The XRD of the Fe^0 before and after used was conducted using an X-ray diffract meter (model D/Max-RC, Japan) to determine the crystalline phases in the catalyst with Cu-Ka radiation in the 2θ range of 10.00–79.98° at a scan rate of 4°/min.

2.4.5. SEM

The surface morphology of the Fe^o before and after use was analyzed by SEM (model S-3400N II/HORIBAEX-250, Japan). The samples were prepared as follows. A small amount of the sample was fixed on a sample table with the use of conductive carbon glue to be pressed flat and dried on the heating plate. An ion sputtering apparatus was used to coat the surface of the sample with platinum to a thickness of 30 angstrom.

3. Results and discussion

3.1. Parameters optimization of the $Fe^o/Na_2S_2O_8$ system in treating leachate biochemical effluent

3.1.1. Effect of $Na_2S_2O_8$ dosage on oxidation performance

When the dosage of Fe^o was 0.5 g/L, pH was 7 and the reaction time was 12 h, the effect of $Na_2S_2O_8$ on the treatment of leachate biochemical effluent was shown in Fig. 1.

As it is shown in Fig. 1, the dosage of $Na_2S_2O_8$ has a significant effect on the removal rate of COD, which was increased with the increase of $Na_2S_2O_8$ dosage. Observing the COD removal curve, it can be seen that the COD removal gradually increased at first and then leveled off with the increasing $Na_2S_2O_8$ dosage. When the dosage of $Na_2S_2O_8$ increased to 2.5 g/L, the COD removal rate reached a maximum at 63%. When the dosage of oxidant continued to increase, the removal of COD did not change clearly and even had a slight trend of decrease. The reason was that the residual persulfate would interfere with COD measurement and the side reaction between $S_2O_8^{2-}\cdot$ and $SO_4^{-}\cdot$ became more significant if continuously increase persulfate concentration [25]. The equation was described as shown in Eq. (1):

$$S_2O_8^{2-}\cdot + SO_4^{-}\cdot \rightarrow S_2O_8^{-}\cdot + SO_4^{2-} \quad k = 6.1 \times 10^5\ M^{-1}\ s^{-1} \tag{1}$$

The removal rate of chroma was relatively low, only about 50%, when the dosage of $Na_2S_2O_8$ was 0.5 g/L. It reached more than 90% and tended to be stable when the dosage of $Na_2S_2O_8$ was 2.0 g/L.

Using $Fe^0/Na_2S_2O_8$ catalytic oxidation system to dispose leachate biochemical effluent, the oxidation reaction was occurred between the produced $SO_4^{-}\cdot$ and the pollutants which came from the leachate biochemical effluent. The quantity of $SO_4^{-}\cdot$ in wastewater was raised with $Na_2S_2O_8$ dosage increasing. This was conducive to the degradation of organic compounds in wastewater samples. The oxida-

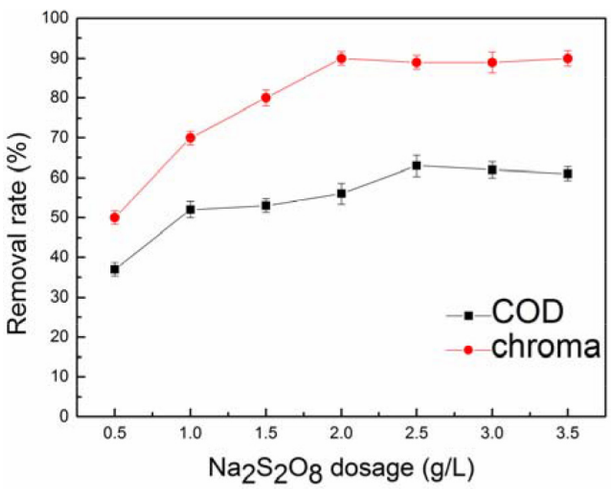

Fig. 1. Effect of $Na_2S_2O_8$ dosage on COD and chroma removal. The initial COD and chroma were 1200 mg/L and 700 times, respectively. (Fe0 dosage = 0.5 g/L, pH=7, reaction time = 12 h).

tion effect was not obvious when the $Na_2S_2O_8$ dosage was more than 2.5 g/L. The reason was that excessive $S_2O_8^{2-}$ in the system may inhibit the generation of $SO_4^{-}\cdot$. On the other hand, the quench reaction would occur between the free $SO_4^{-}\cdot$ and lead to invalid consumption [26]. Taking the variation of leachate biochemical effluent wastewater quality into consideration in the practical application, when the COD of effluent was 700–1300 mg/L, it was best to select the 2.5 g/L $Na_2S_2O_8$ dosage as the optimal dosage from the economic point of view.

3.1.2. Effect of Fe^0 dosage on oxidation performance

When the dosage of $Na_2S_2O_8$ was 2.5 g/L, pH was 7 and reaction time was 12 h, the effect of Fe^0 dosage on the treatment of leachate biochemical effluent is shown in Fig. 2.

Observing the COD removal curve, it can be seen that the removal rate of COD increased rapidly at first with the increase of Fe^0 dosage. When the dosage was 0.2 g/L, the removal rate of COD was 49%. When the dosage increased to 0.5 g/L, the removal rate of COD reached its highest at 62%. However, the removal of COD decreased when the dosage of Fe^0 continued to increase. This was mainly due to the fact that the Fe^0 was the continuous supply source of Fe^{2+}, and the concentration of Fe^{2+} in wastewater would increase if increasing the dosage of Fe^0 appropriately, making the-O-O- bond in $S_2O_8^{2-}$ broken and $SO_4^{-}\cdot$ generated [27], which greatly improved oxidation effect of pollutants in wastewater. Certainly, COD and chroma removal rate also rose. But the removal rate of COD had a trend to decrease with sustained increasing of the Fe^0 dosage. The reason was that, overdosing Fe^0 would increase the concentration of Fe^{2+} and generate excessive $SO_4^{-}\cdot$, which can have a quenching reaction between each other, reduce the oxidation-reduction potential in water. A vicious phenomenon arose due to the reaction between a great deal of Fe^{2+} and the $SO_4^{-}\cdot$ at the same time, which can be described as shown in Eq. (2):

$$SO_4^{-}\cdot + Fe^{2+} \rightarrow SO_4^{2-} + Fe^{3+} \quad (2)$$

This reaction would lead to some problems, such as: the reduction of oxidant and catalyst utilization ratio, the increase of treatment cost and the deterioration of oxidation system. Observing the chroma removal curve, when the Fe^0 dosage was more than 0.2 g/L, the removal rate of chroma approached 50%. It reached about 91% at 0.5 g/L dosage, and then the removal of chroma on a downward trend with the increased dosage of Fe°. It was because that chroma interference was happened by lots of Fe^{2+} and Fe^{3+} which were generated by overdosing Fe^0. It was also necessary to control the dosage of Fe^0 reasonably in the engineering application according to the characteristics of wastewater, because overdosing Fe^0 can not only raise the cost, but also enhance the chroma of effluent which was due to residual iron in wastewater.

3.1.3. Effect of pH value on oxidation performance

Under the conditions as follows: the dosage of $Na_2S_2O_8$ was 2.5 g/L, the dosage of Fe^0 was 0.5 g/L and the reaction time was 12 h, the effect of pH value on the treatment of leachate biochemical effluent was shown in Fig.3.

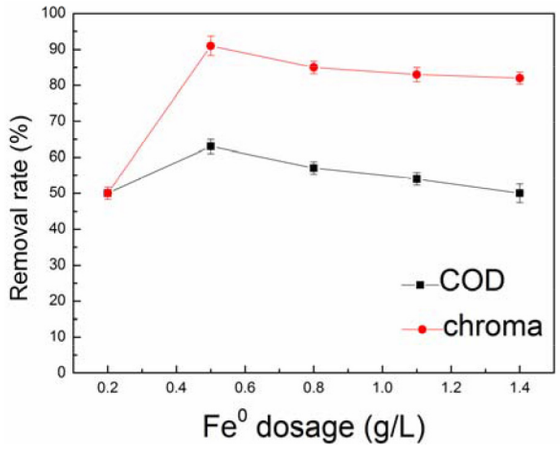

Fig. 2. Effect of Fe^0 dosage on COD and chroma removal ($Na_2S_2O_8$ dosage = 2.5 g/L, pH = 7, reaction time = 12 h).

The results can be concluded from the Fig. 3, when the pH value was lower than 7, the removal of COD increased with the rise of the pH value. But it reached its maximum at 71% when the pH value was around neutral. Continued to grow the pH until it's alkaline, the removal rate of COD started decreasing. However, the chroma removal rate reached a maximum at 95% when the pH was 3. The reason was that Fe^{2+} was generated by the reaction between a larger quantity of Fe^0 and acid under the condition of strong acid. The reaction can cause high concentration of Fe^{2+} in the wastewater, and side reaction would happen as shown in Eq. (1) in section 3.1.2.

The reaction above not only consumed a great deal of Fe^0 and the oxidant of sodium persulfate, resulting in the cost rise, but also weakened the oxidation system, making the COD removal rate cannot reach the best under the acidic conditions. It is optimal for the removal rate of COD when the pH value is neutral. Because in this condition the release rate of Fe^{2+} was moderate, without a side reaction caused by the high concentration of Fe^{2+} in a short time. However, the removal rate of COD was sequentially declined under the condition of alkalescence, the primary reasons were as follows: under the alkalinity condition, first, the concentration of Fe^{2+} in wastewater was at a low level due to the generation of ferrous hydroxide sediment; second, many metal ion precipitations were attached to the surface of Fe^0 and made it difficult to oxidize into Fe^{2+} for the ability of electron transfer losing; third, the active substance of $SO_4^{-}\cdot$ was quickly quenched because of the reaction between the $SO_4^{-}\cdot$ and hydroxyl ions in the solution; last, under the circumstances of weak alkaline, there existed lots of HCO_3^- and CO_3^{2-} in the solution, which can react with $SO_4^{-}\cdot$, making its concentration decreased for the vicious competition. The treatment efficiency in the pH 11 was better than that in pH 9 under the alkaline condition. The reason was maybe that the free radicals which played a main role in the oxidation process would change if the pH value in the Fe^0/$Na_2S_2O_8$ system changed. Under acid conditions, the dominant role of the system was $SO_4^{-}\cdot$. While the pH value was

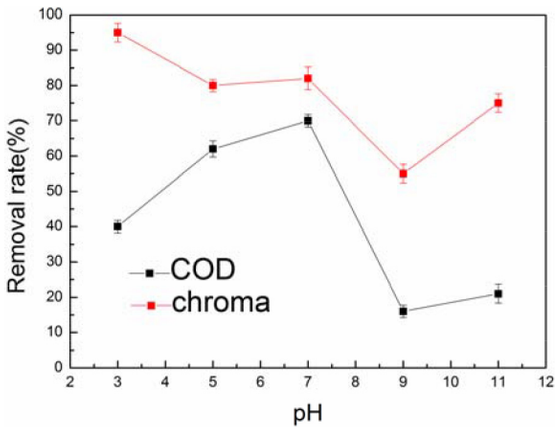

Fig. 3. Effect of pH on the COD and chroma removal ($Na_2S_2O_8$ dosage = 2.5 g/L, Fe^0 dosage = 0.5 g/L, reaction time = 12 h)

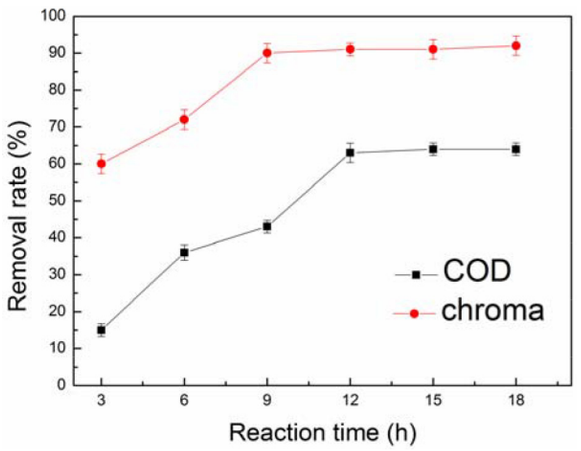

Fig. 4. Effect of reaction time on COD and chroma removal ($Na_2S_2O_8$ dosage = 2.5 g/L, Fe^0 dosage = 0.5 g/L, pH= 7).

greater than 10, the degradation of organic contaminants in the solution was mainly depended on ·OH. However, the amount of ·OH generated under alkaline conditions was so limited that the removal efficiency of COD and chroma would not be improved rapidly with the increase of pH [28].

3.1.4. Effect of reaction time on oxidation performance

When the dosage of $Na_2S_2O_8$ was 2.5 g/L, pH was 7 and the dosage of Fe^0 was 0.5 g/L, the effect of reaction time on treatment of leachate biochemical effluent is shown in Fig. 4.

As can be observed in Fig. 4, the removal rate of COD and chroma rose fleetly with the reaction time prolonging and then tended to be a balance little by little. When the reaction time achieved 12 h, the removal rate of COD and chroma reached 56% and 93%, respectively. Then with the reaction time continuing to extend, the chroma removal rate tended to be gradually stabilized, while the COD removal rate had a slight increase. It can be concluded that the oxidation reaction was almost over in the reaction time of 12 h. When the reaction time was 4 h, the chroma removal rate was as high as 73%, indicating that the chroma removal was accomplished substantially by the $Fe^0/Na_2S_2O_8$ system in a short time. The main reason was that the sulfate radicals would attack on the chromogenic substances first when it was in the offensive of polluted organic matters, making the removal rate of chroma reached an ideal effect in a short oxidation reaction time, and it basically tended to be stability when the time was 10 h. Sulfate radical is a kind of free radical with strong oxidation ability, which can not only split the carbon chains of organic matters in the wastewater, but also decompose the macromolecular organic compounds that are difficult to be degraded into small molecule organic matters which is easy to be biodegradable, or completely mineralized into carbon dioxide and water. For this reaction, the sulfate radicals production was a slow release progress which was favorable for the reaction of SO_4^{-}· and contaminants [29]. While, dosing Fe^{2+} directly would easily cause the Fe^{2+} amounts in the oxidation system to be more excessive than that required for activation reaction. This can conduct side reaction between Fe^{2+} and generated SO_4^{-}·, and can consume SO_4^{-}· ineffectively, which lead to a low oxidation efficiency [30,31].

3.2. Analysis of wastewater quality before and after treatment

3.2.1. Analysis of wastewater samples before and after treatment with 3DEEMFS

3DEEMFS was used to elucidate the nature of DOM (dissolved organic matter) from the three-dimensional fluorescent fingerprints [32]. The fluorescence spectra of the leachate biochemical effluent and $Fe^0/Na_2S_2O_8$ effluent are shown in Fig. 5. In order to prevent the effect of internal filtering, the determination wastewater samples have been diluted 10 times.

As shown in Fig. 5a, there were three peaks (A = E_x/E_m = 255 nm/465 nm, B = E_x/E_m = 285 nm/430 nm, C = E_x/E_m = 330 nm/430 nm) of DOM in leachate biochemical effluent. Each intensity of fluorescence was 2154, 1684 and 1832, respectively. According to the research, it showed that the fluorescence peak appeared in the area of E_x/E_m = (250 nm~390 nm)/(370 nm~480 nm), which implied that there existed humic substances in wastewater. The fluorescence peak center appeared in the area of E_x/E_m = (280 nm~370 nm)/(380 nm~460 nm), indicating that the wastewater sample contained fulvic acid and humic acid. The fluorescence peak center appeared in the area of E_x/E_m = (310 nm~360 nm)/(370 nm~450 nm), which showed the existence of fulvic acid in the wastewater sample. Regarding the effluent of the $Fe^0/Na_2S_2O_8$ system, it can be seen from Fig.5b that the fluorescence peaks mainly appeared in the positions as follows: D = E_x/E_m = 240 nm/395 nm, E = E_x/E_m = 280 nm/360 nm and F = E_x/E_m = 330 nm/405 nm, and the intensity of peak were 679.6, 470.5 and 634.2, respectively. Furthermore, there was UV fulvic acid in the wastewater when the fluorescence peak appeared in the area of E_x/E_m = (240 nm~270 nm)/(370 nm~440 nm). The fluorescence peak appeared in the area of E_x/E_m = (310 nm~360 nm)/(370 nm~450 nm), indicating that there existed the visible fulvic acid in the water.

According to the above analyses, it can be known that the leachate treated with the $Fe^0/Na_2S_2O_8$ system no longer contained a large amount of humic acid substances with the characteristics of high molecular weight, high degree of aromatic structure, complex molecular structure. But after the

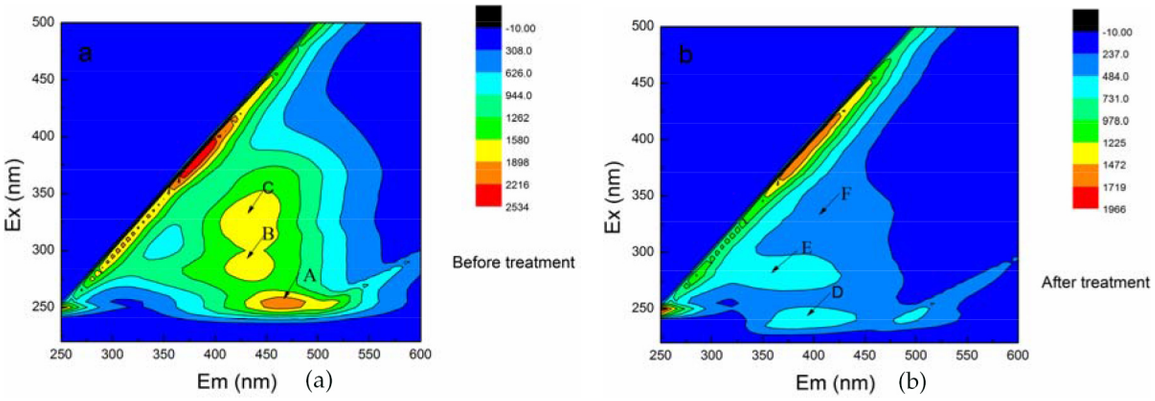

Fig. 5. 3DEEMFS of wastewater samples before and after treatment.

treatment of the $Fe^0/Na_2S_2O_8$ system, the complex humic acid was oxidized into fulvic acid by $SO_4^{-}\cdot$ which had the characteristics of lower molecular weight, lower degree of aromatization and simple molecular structure. Comparing with the fluorescence peak intensity of fulvic acid area before and after the treatment by the $Fe^0/Na_2S_2O_8$ system, it can be seen that the fluorescence peak intensity decreased from 1382 to 470, and the degradation rate reached 66%, which was tally with the COD removal. The results indicated that the $Fe^0/Na_2S_2O_8$ system had the ability of effective removal on fulvic acid. After the treatment of the $Fe^0/Na_2S_2O_8$ system, the emission wavelength of fulvic acid in the visible light area showed significantly blue-shift from 430 nm to 405 nm, owing to the decrease of the conjugation of the dissolved organic compounds molecules and the reduction of molecular condensation degree in the wastewater. It can be found from the entire fluorescence spectrum that a decrease in fluorescence intensity, which indicated the reduction in the level of organic contaminants.

The fluorescence index $f_{450/500}$ had a certain relationship with the aromaticity of fulvic acid in the wastewater. The larger the fluorescence index, the worse the aromaticity of fulvic acid in the wastewater. The fluorescence index of untreated leachate biochemical effluent was 1.37. The aromaticity of dissolved fulvic acid was strong, owing to the aromatic ring structure. The $f_{450/500}$ of dissolved fulvic acid in the wastewater sample treated with the $Fe^0/Na_2S_2O_8$ activation system was 2.01, indicating that the aromaticity of dissolved humic acid weakened and the aromatic ring structure reduced. The humic acid in wastewater was oxidized by the $Fe^0/Na_2S_2O_8$ system from the above analyses.

3.2.2. *Analysis of wastewater samples before and after treatment with UV-vis*

The ultraviolet absorption of DOM is related to the unsaturated conjugate bond of the compound according to the strong absorbance in the ultraviolet area [33]. As can be seen from Fig. 6, comparing with the UV-vis absorbance value before treatment, the value of that in the leachate biochemical effluent sample has dropped massively after treatment with the $Fe^0/Na_2S_2O_8$ system when they were at the same wavelength. It illustrated that the oxidation system can not only greatly remove the organic matter in wastewater, but also can gradually decrease the complexity and aromaticity of molecular. Observing the UV-vis absorption curve, it can be seen that the absorbency has been showing a decreasing trend with the increase of wavelength, and finally reducing to zero. Owing to the complexity of leachate wastewater quality, there was no occurrence of massive absorption peaks throughout the whole UV absorption band. Nevertheless, it can be found from the Fig. 6 that when the wavelength was greater than 250 nm, the wastewater sample treated with the $Fe^0/Na_2S_2O_8$ system no longer had absorbance, which proved once more that the organic matter content and types of the treated wastewater samples evidently reduced comparing with those of the raw wastewater samples [34,35].

3.2.3. *Analysis of wastewater samples before and after treatment with FTIR*

According to the relevant literature, the absorbance bands appeared at 3467 cm^{-1} was stretching vibration area of hydroxyl or carboxyl. Those near 1635 cm^{-1} bands corresponded to skeleton vibration peaks of C=C on the benzene ring. The area at 1382 cm^{-1} corresponded to the out-of-plane C-H bends vibration of a saturated hydrocarbon. The absorption bands around 1090 cm^{-1} indicated that there existed polysaccharides, carboxylic acids and alcohols in the wastewater sample. The area 615 cm^{-1} was corresponded to the out-of-plane bend of C-N, N-H, and C-H of the benzene ring [36,37].

The FTIR spectra of wastewater samples before and after treatment were shown in Fig. 7. It can be found from Fig. 7 that there were both strong characteristic bands before and after treatment of wastewater samples on the area near 3411 cm^{-1}, which indicated there existed carboxyl or hydroxyl in DOM in the wastewater samples [37,38]. There were both characteristic peaks before and after treatment of wastewater samples on the area near 1635 cm^{-1}, which indicated that the wastewater samples contained aromatic substances [37]. However, the intensity of the treated wastewater sample at this band sharply declined compared with that of the raw wastewater. Because some aromatic substances were translated to substance with smaller molecules by $SO_4^{-}\cdot$

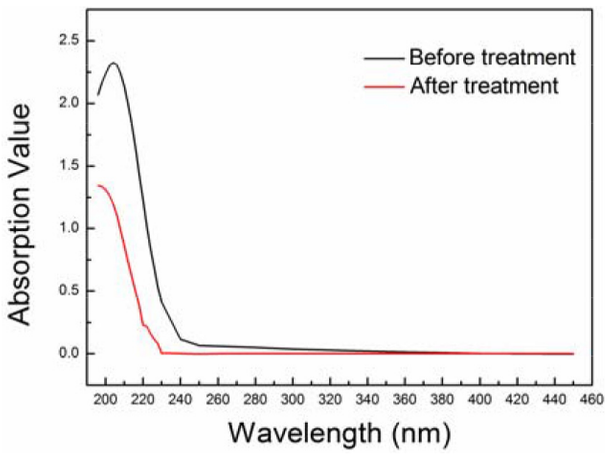

Fig. 6. UV-vis absorption spectra of wastewater samples before and after treatment.

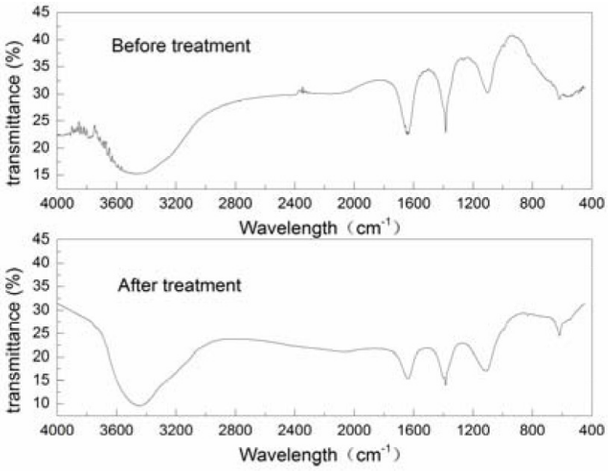

Fig. 7. FTIR spectra of wastewater samples before and after treatment.

oxidation and the aromaticity of organics was weakened. As shown in Fig. 7, the characteristic peak at 1386 cm^{-1} disappeared after treatment for the reason that the carboxylic groups were cleaved by sulfate radicals, resulting in the generation of organics with worse stability and smaller relative molecular weight. The intensity at bands 1090 cm^{-1} declined remark ablely in the wastewater sample treated with the $Fe^0/Na_2S_2O_8$ system, which indicated that polysaccharide and carboxylic acids were oxidized by the SO_4^{-}·. It can also be deduced that the relative reduction in protein was from the great reduction of the intensity of characteristic bands at 620 cm^{-1}. A weak absorbance band at 590 cm^{-1} emerged in the treated wastewater sample, illustrating the presence of Fe-O bond stretching vibration and iron compounds [39]. In whole, the molecular structure of the macromolecular organic compounds became more unstable and the molecular weight became smaller after treatment of the oxidation system. Meanwhile, small molecule substance was oxidized into carbon and water via the $Fe^0/Na_2S_2O_8$ system. The organics in wastewater had a decrease because of both a certain change in the structure and some decreases in intensity of functional group.

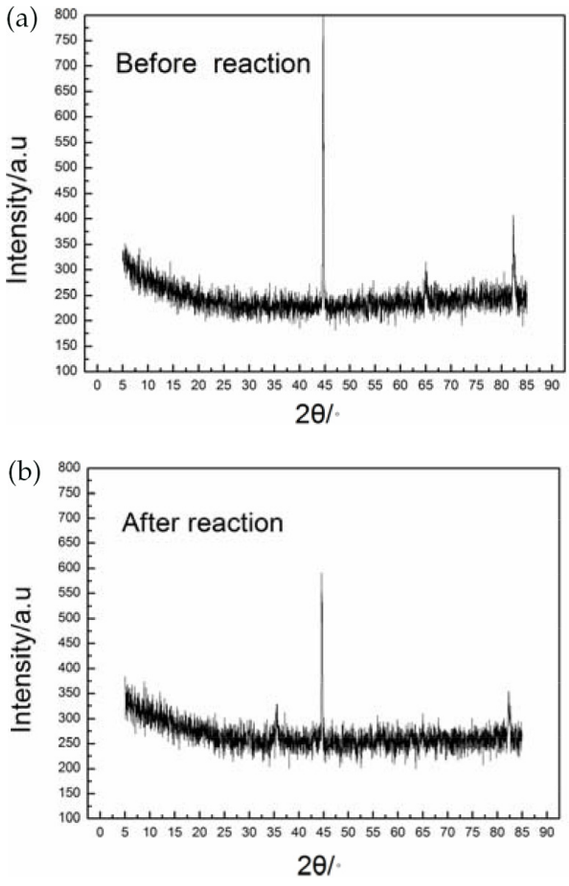

Fig. 8. The Fe^0 XRD spectra before and after reaction.

3.3. Characterization and analysis of catalysts

3.3.1. XRD characterization of ZVI before and after reaction

The XRD patterns of Fe^0 (before and after reaction) are shown in Fig. 8. It can be seen that the characteristic peaks (2θ) of Fe^0 before reaction appeared at 44.7°, 65°, and 82° respectively, which are almost the same as the standard spectra for ferrum (Joint Committee on Powder Diffraction System, JCPDS NO.656212). This showed that the Fe^0 before reaction was pure without impurities, and there was no occurrence of oxidation reaction. After reaction, the characteristic peaks (2θ) of ZVI appeared at 35.1°, indicating that the characteristic peaks of Fe_3O_4 appeared in the Fe^0. Also, there were not only Fe^0 but also Fe^{2+} and Fe^{3+} absorbed on the surface of Fe^0 after reaction. This is consistent with the mechanism of treating wastewater by Fe^0 catalyzing persulfate [40]. The Fe^0 diffraction intensity was significantly decreased after the reaction. It was likely owing to the occurrence of Fe^0 agglomeration as well as the adsorption of some pollutants on the Fe^0 surface, which made the inter

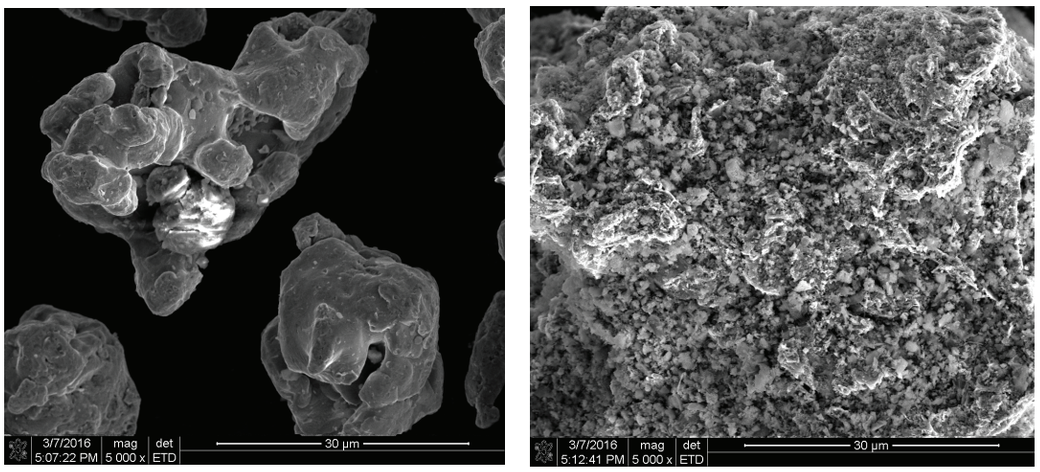

Before reaction After reaction

Fig. 9. SEM micro graph of Fe^0 before and after reaction.

space among Fe^0 become smaller. The diffraction peaks of Fe^0 became more flat and peaks value also decreased after reaction, so it could be deduced that the diameter of Fe^0 became smaller.

3.3.2. SEM characterization of Fe^0 before and after reaction

The SEM micrograph of Fe^0 (before and after reaction) was shown in Fig. 9. It can be seen that the Fe^0 (before reaction) was loose and there was no occurrence of agglomeration. According to the size of the micro graph, it can be roughly estimated that the diameter of the Fe^0 particles is about 30 µm. After reaction, the surface of Fe^0 gradually became smooth from irregular uneven because a large quantity of snowflake-like iron oxides was attached on it. It can be inferred that the Fe^0 was oxidized into Fe_3O_4, a-Fe_3O_2, a-FeOOH by the persulfate from the presence of snowflake-like iron oxides. This conclusion confirmed the result of XRD detection.

4. Conclusion

In this work, the application of sulfate radical oxidation based on Fe^0 activation for leachate biochemical effluent was studied, and it was proved to be an efficient and promising method. The oxidation efficiencies were affected by the factors of $Na_2S_2O_8$ dosage, Fe^0 dosage, wastewater pH, and reaction time. With 2.5 g/L $Na_2S_2O_8$ dosage and 0.5 g/L Fe^0 dosage, the COD and chroma removals can reach up to 71% and 90%, respectively, after the 12 h treatment.

It can be concluded from 3DEEMFS that the most of humic acid substances were oxidized and removed, and fulvic acid was degraded effectively of which the removal rate reached 66%, when the leachate biochemical effluent was treated with the $Fe^0/Na_2S_2O_8$ system. Making a comparison of the fluorescence index ($f_{450/500}$) before and after treatment, it was found that the aromaticity of the soluble humic acid was weakened, and the structure of the aromatic ring was reduced as well. UV-vis spectra analyses indicated that after the treatment of $Fe^0/Na_2S_2O_8$ system, the degree of organic pollution was decreased significantly and the substituted groups of dissolved organic matter (DOM) were also lessened. Moreover, the stability of organic matter changed to be worse due to the main structure of fat chains. According to FTIR spectroscopy, the macromolecular organic matter in the leachate biochemical effluent was decomposed into small molecular organic matter, the organic functional groups and structure also had some changes, and the stability of dissolved organic matter structure was decreased.

XRD patterns analyses showed that the characteristic peaks of Fe_3O_4 appeared in the Fe^0, indicating not only Fe^0 but also Fe^{2+} and Fe^{3+} absorbed on the surface of Fe^0 after the reaction. Moreover, the diffraction peaks of Fe^0 became more flat and peaks value also decreased after reaction, owing to the occurrence of Fe^0 agglomeration as well as the adsorption of some pollutants on the Fe^0 surface. According to the SEM micro graph of Fe^0 (before and after reaction), the surface of Fe^0 gradually became smooth from irregular uneven and with a large quantity of snowflake-like iron oxides attached to it.

Acknowledgements

This work was supported by the National Natural Sciences Foundation of China (No. 51468016 and No. 61640217), the Natural Sciences Foundation of Jiangxi (No. 20171BAB206047), the Technology Development Research Project of Jiangxi (No. 20171BBH80008), and the achievement transformation project of Jiangxi (No. 20161BBI90033).

References

[1] K. Mahmud, M.D. Hossain, S. Shams, Different treatment strategies for highly polluted landfill leachate in developing countries, Waste Manage., 32 (2012) 2096–2105.
[2] E. Turro, A. Giannis, R. Cossu, E. Gidarakos, D. Mantzavinos, A. Katsaounis, Electrochemical oxidation of stabilized landfill leachate on DSA electrodes, J. Hazard. Mater., 190 (2011) 460–465.

[3] A. Fernandes, P. Spranger, A.D. Fonseca, M.J. Pacheco, L. Ciríaco, A. Lopes, Effect of electrochemical treatments on the biodegradability of sanitary landfill leachates, Appl. Catal. B, 144 (2014) 514–520.
[4] X.-Y. Xu, G.-M. Zeng, Y.-R. Peng, Z. Zeng, Potassium persulfate promoted catalytic wet oxidation of fulvic acid as a model organic compound in landfill leachate with activated carbon, Chem. Eng. J., 200–202 (2012) 25–31.
[5] P. Wang, G. Zeng, Y. Peng, F. Liu, C. Zhang, B. Huang, Z. Yu, Y. He, M. Lai, 2,4,6-Trichlorophenol-promoted catalytic wet oxidation of humic substances and stabilized landfill leachate, Chem. Eng. J., 247 (2014) 216–222.
[6] Y.C. Chou, S.L. Lo, J. Kuo, C.J. Yeh, Derivative mechanisms of organic acids in microwave oxidation of landfill leachate, J. Hazard. Mater., 254–255 (2013) 293–300.
[7] M. Chys, V.A. Oloibiri, W.T.M. Audenaert, K. Demeestere, S.W.H. Van Hulle, Ozonation of biologically treated landfill leachate: efficiency and insights in organic conversions, Chem. Eng. J., 277 (2015) 104–111.
[8] A. Amiri, M.R. Sabour, Multi-response optimization of Fenton process for applicability assessment in landfill leachate treatment, Waste Manage., 34 (2014) 2528–2536.
[9] T.F. Silva, R. Ferreira, P.A. Soares, D.R. Manenti, A. Fonseca, I. Saraiva, R.A. Boaventura, V.J. Vilar, Insights into solar photo-Fenton reaction parameters in the oxidation of a sanitary landfill leachate at lab-scale, J. Environ. Manage., 164 (2015) 32–40.
[10] A. Anfruns, J. Gabarro, R. Gonzalez-Olmos, S. Puig, M.D. Balaguer, J. Colprim, Coupling anammox and advanced oxidation-based technologies for mature landfill leachate treatment, J. Hazard. Mater., 258–259 (2013) 27–34.
[11] Y. Ji, Y. Fan, K. Liu, D. Kong, J. Lu, Thermo activated persulfate oxidation of antibiotic sulfamethoxazole and structurally related compounds, Water Res., 87 (2015) 1–9.
[12] S. Yang, X. Yang, X. Shao, R. Niu, L. Wang, Activated carbon catalyzed persulfate oxidation of Azo dye acid orange 7 at ambient temperature, J Hazard. Mater., 186 (2011) 659–666.
[13] J. Sharma, I.M. Mishra, D.D. Dionysiou, V. Kumar, Oxidative removal of Bisphenol A by UV-C/peroxy mono sulfate (PMS): Kinetics, influence of co-existing chemicals and degradation pathway, Chem. Eng. J., 276 (2015) 193–204.
[14] Y.C. Chou, S.L. Lo, J. Kuo, C.J. Yeh, A study on microwave oxidation of landfill leachate--contributions of microwave-specific effects, J. Hazard. Mater., 246–247 (2013) 79–86.
[15] Y.C. Chou, S.L. Lo, J. Kuo, C.J. Yeh, Microwave-enhanced persulfate oxidation to treat mature landfill leachate, J. Hazard. Mater., 284 (2015) 83–91.
[16] Y. Fan, Y. Ji, D. Kong, J. Lu, Q. Zhou, Kinetic and mechanistic investigations of the degradation of sulfamethazine in heat-activated persulfate oxidation process, J. Hazard. Mater., 300 (2015) 39–47.
[17] I. Epold, N. Dulova, Oxidative degradation of levofloxacin in aqueous solution by $S_2O_8^{2-}/Fe^{2+}$, $S_2O_8^{2-}/H_2O_2$ and $S_2O_8^{2-}/OH^-$ processes: A comparative study, J. Environ. Chem. Eng., 3 (2015) 1207–1214.
[18] F. Fu, D.D. Dionysiou, H. Liu, The use of zero-valent iron for groundwater remediation and wastewater treatment: a review, J. Hazard. Mater., 267 (2014) 194–205.
[19] D.-L. Huang, G.-M. Chen, G.-M. Zeng, P. Xu, M. Yan, C. Lai, C. Zhang, N.-J. Li, M. Cheng, X.-X. He, Y. He, Synthesis and Application of Modified Zero-Valent Iron Nano particles for Removal of Hexavalent Chromium from Wastewater, Water Air Soil Pollut., 226 (2015).
[20] M. Nilsson, L. Andreas, A. Lagerkvist, Effect of accelerated carbonation and zero valent iron on metal leaching from bottom ash, Waste Manage., 51 (2016) 97–104.
[21] A.A. And, P.G. Tratnyek, Reduction of nitro aromatic compounds by zero-valent iron metal, Environ. Sci. Technol., 30 (1995) 153–160.
[22] S.Y. Oh, H.W. Kim, J.M. Park, H.S. Park, C. Yoon, Oxidation of polyvinyl alcohol by persulfate activated with heat, Fe^{2+}, and zero-valent iron, J. Hazard. Mater., 168 (2009) 346–351.
[23] C. Liang, C.J. Bruell, M.C. Marley, K.L. Sperry, Persulfate oxidation for in situ remediation of TCE. I. Activated by ferrous ion with and without a persulfate-thiosulfate redox couple, Chemosphere, 55 (2004) 1213–1223.
[24] S.Y. Oh, S.G. Kang, P.C. Chiu, Degradation of 2,4-dinitrotoluene by persulfate activated with zero-valent iron, The Sci. Total Environ., 408 (2010) 3464–3468.
[25] H. Zhang, Z. Wang, C. Liu, Y. Guo, N. Shan, C. Meng, L. Sun, Removal of COD from landfill leachate by an electro/Fe^{2+}/peroxydisulfate process, Chem. Eng. J., 250 (2014) 76–82.
[26] J. Zeng, L. Hu, X. Tan, C. He, Z. He, W. Pan, Y. Hou, D. Shu, Elimination of methyl mercaptan in ZVI-$S_2O_8^{2-}$ system activated with in-situ generated ferrous ions from zero valent iron, Catal. Today, 281 (2017) 520–526.
[27] A. Ahmad, X. Gu, L. Li, S. Lu, Y. Xu, X. Guo, Effects of pH and anions on the generation of reactive oxygen species (ROS) in nZVI-rGo-activated persulfate system, Water Air Soil Pollut., 226 (2015) 369–381.
[28] K.-C. Huang, R.A. Couttenye, G.E. Hoag, Kinetics of Heat-Assisted Persulfate Oxidation of Methyl tert -Butyl Ether (MTBE), Soil Sediment Contam., 11 (2002) 447–448.
[29] A. Romero, A. Santos, F. Vicente, C. González, Diuron abatement using activated per-sulphate: Effect of pH, Fe (II) and oxidant dosage, Chem. Eng. J., 162 (2010) 257–265.
[30] J. Zhao, Y. Zhang, X. Quan, S. Chen, Enhanced oxidation of 4-chlorophenol using sulfate radicals generated from zero-valent iron and peroxydisulfate at ambient temperature, Sep. Purif. Technol., 71 (2010) 302–307.
[31] H. Li, J. Wan, Y. Ma, Y. Wang, M. Huang, Influence of particle size of zero-valent iron and dissolved silica on the reactivity of activated persulfate for degradation of acid orange 7, Chem. Eng. J., 237 (2014) 487–496.
[32] X. Zhao, X. Wei, P. Xia, H. Liu, J. Qu, Removal and transformation characterization of refractory components from biologically treated landfill leachate by Fe^{2+}/NaClO and Fenton oxidation, Sep. Purif. Technol., 116 (2013) 107–113.
[33] Y.P. Chin, G. Aiken, E. O'Loughlin, Molecular weight, polydispersity, and spectroscopic properties of aquatic humic substances, Environ. Sci. Technol., 28 (1994) 1853–1858.
[34] G.B.R. Artinger, S. Geyer, P. Fritz, M. Wolf, J.I. Kim Characterization of groundwater humic substances: influence of sedimentary organic carbon, Appl. Geochem., 15 (2000) 97–116.
[35] H.S.S. Ki-Hoon Kang, H. Park, Characterization of humic substances present in landfill leachates with different landfill ages and its implications, Water Res., 36 (2002) 4023–4032.
[36] L. Zhang, A. Li, Y. Lu, L. Yan, S. Zhong, C. Deng, Characterization and removal of dissolved organic matter (DOM) from landfill leachate rejected by nano filtration, Waste Manage., 29 (2009) 1035–1040.
[37] G. Zhang, Y. Jiao, D.J. Lee, Transformation of dissolved organic matters in landfill leachate-bio electro chemical system, Bio resour Technol., 191 (2015) 350–354.
[38] Z. Liu, W. Wu, P. Shi, J. Guo, J. Cheng, Characterization of dissolved organic matter in landfill leachate during the combined treatment process of air stripping, Fenton, SBR and coagulation, Waste Manage., 41 (2015) 111–118.
[39] M. Gotić, S. Musić, Mössbauer, FT-IR and FE SEM investigation of iron oxides precipitated from $FeSO_4$ solutions, J. Mol. Struct., 834–836 (2007) 445–453.
[40] I. Grčić, S. Papić, K. Žižek, N. Koprivanac, Zero-valent iron (ZVI) Fenton oxidation of reactive dye wastewater under UV-C and solar irradiation, Chem. Eng. J., 195–196 (2012) 77–90.